CrossMark

# Shape-Dependent Magnetic Properties and Phase Transformation of Annealed Iron Oxide Nanoparticles

SAMIRA NAGHDI,[1] KYONG YOP RHEE,[1,3] and SOO JIN PARK[2,4]

1.—Department of Mechanical Engineering, College of Engineering, Kyung Hee University, Yongin 446-701, Korea. 2.—Department of Chemistry, Colloge of Natural Science, Inha University, Incheon 402-751, Korea. 3.—e-mail: rheeky@khu.ac.kr. 4.—e-mail: sjpark@inha.ac.kr

After investigation of different methods to synthesize magnetic nanoparticles (MNPs), finding methods to control their magnetic properties and to optimize their characteristics remains challenging. Heat treatment has been introduced as a perfect method that can affect the shape and size of MNPs and thus their magnetic properties. In this work, iron oxide ($Fe_2O_3$) nanoparticles with various shapes were produced by means of a microwave-assisted method, with use of cost-effective and non-toxic chemicals. These particles were then annealed at different temperatures, i.e., 300°C, 500°C, and 800°C, for 2 h in the presence of air. The results indicated that heated samples exhibited weaker magnetic properties than those of non-heated samples. Both x-ray diffraction and Raman analysis results of the annealed samples indicated that the $Fe_2O_3$ particles were well crystalline, with transformation in phases. Transmission electron microscopy images indicated that all the annealed particles were spherical, regardless of their initial shapes.

## INTRODUCTION

In recent decades, nanoparticles (NPs) of magnetic metals and oxides have attracted scientific interest because of their excellent biocompatibility and magnetic properties.[1,2] Synthesized magnetic nanoparticles (MNPs) are a class of NPs that react to applied magnetic fields. Usually, MNPs contain magnetic elements such as iron, cobalt and nickel, and include different chemical compounds of these elements.[3] Because of their enormous potential applications, various MNPs have been synthesized and used in different research areas, including catalysis, microfluidics, magnetic particle imaging, magnetic resonance imaging, data storage, nanofluids, defect sensing, biotechnology, biomedicine and optical filtering.[4–7] Among the various MNPs, iron oxide ($Fe_2O_3$) has attracted the most attention because of its importance and vast applicability in industry, medical science and research.[2,7,8] There has been a great deal of research on MNPs, but finding methods to change and control their magnetic properties and to optimize their characteristics remains challenging. In some works, these aspects have been controlled by changing the shape, size, structure and chemical composition of the

MNPs.[9] Recently, thermal annealing has been introduced as a perfect method that can affect the shape and size of MNPs and thus their magnetic properties.[10] Also, heat treatment of MNPs changes their crystal structure. Heat treatment can change amorphous or imperfectly crystalline materials into materials with larger or more perfect crystalline structures.[11–21] Yufanyi et al.[14] investigated the effects on $\alpha$-$Fe_2O_3$ NPs of heat treatment at 300°C, 400°C and 500°C for 2 h, and found that annealed $\alpha$-$Fe_2O_3$ NPs varied in crystallinity with the variation in the heat treatment temperature used. Xu et al.[15] annealed $Fe_2O_3$ NPs in air and in vacuum, with the phase transformation of NPs into $\alpha$-$Fe_2O_3$ occurring directly during annealing in air, and also occurring during annealing in vacuum at temperatures higher than 450°C. We have previously reported the synthesis of $Fe_2O_3$ NPs by means of a microwave-assisted method and have presented experimental results related to $Fe_2O_3$ NPs of different sizes, morphologies and magnetic properties that can be obtained by using different concentrations of urea.[7] However, the $Fe_2O_3$ NPs discussed in the previous report were of two mixed phases ($\alpha$- and $\gamma$-$Fe_2O_3$) and exhibited poor crystallinity. In the present study, we continued our investigation of $Fe_2O_3$

NPs. We heated different $Fe_2O_3$ NPs having different particle shapes and sizes in air at 300°C, 500°C, and 800°C. Here, we focus on three aspects: first, the influence of heat treatment upon crystal structure and phase transformation; second, the variation of the magnetic properties of $Fe_2O_3$ NPs caused by heat treatment; and finally, changes in the shape and size of $Fe_2O_3$ NPs.

## EXPERIMENTAL

The synthesis of $Fe_2O_3$ NPs was carried out in a similar manner as in our previous work.[7] Iron(III) chloride ($FeCl_3$, 97%; Sigma Aldrich, Germany) and urea (98.0%; Dae Jung, South Korea) were used as the raw materials in this experiment. For the synthesis of the samples, a 700-W microwave oven (Samsung, RE-MP20) was utilized. For preparation of the $Fe_2O_3$ with different morphologies, different amounts of urea was used: 1 g of urea was used to prepare a sample termed $F_1$; other samples ($F_0$, $F_5$ and $F_{10}$) were prepared by means of the same procedure but using different amounts of urea (0 g for sample $F_0$, 5 g for sample $F_5$ and 10 g for sample $F_{10}$). After preparation of the samples, x-ray diffraction analysis (XRD; Bruker D8 Advance; x-ray source: Cu $K\alpha_1$, $\lambda$ = 1.5406 Å) was used for investigation of the crystal structures of the samples. FT-Raman spectra were acquired using a Bruker RFS100/S instrument. Fourier transform infrared

spectroscopy (FTIR) was obtained using a Spectrum One system (Perkin-Elmer) spectrometer. The morphology of the samples was investigated using a transmission electron microscope (TEM; JEM-2100F instrument). The magnetic properties of the $Fe_2O_3$ NPs were characterized by means of a vibrating sample magnetometer (VSM; Lake Shore 7300) with magnetic field strengths up to 10 kOe.

## RESULTS AND DISCUSSION

### XRD Analysis

XRD patterns were acquired for the as-prepared and annealed MNPs at various temperatures (Fig. 1). Similar to findings in our previous work, XRD patterns of the as-prepared $Fe_2O_3$ NPs indicated that they were composed of hematite and maghemite phases and were of poor crystallinity. Furthermore, with increasing urea concentration (from 1 g to 10 g), the XRD peak intensity also increased. After heat treatment of the as-prepared samples in air at 300°C, the positions of all the diffraction peaks matched those characteristic of the hematite phase (JCPDS card 13-0534). Before heat treatment, both hematite and maghemite phases were present in the samples' diffraction patterns.[7] Contrastingly, after heat treatment, the samples had undergone a phase transformation to $\alpha$-$Fe_2O_3$, the most thermodynamically stable $Fe_2O_3$.[20,22] Heat treatment at 300°C completely transformed the
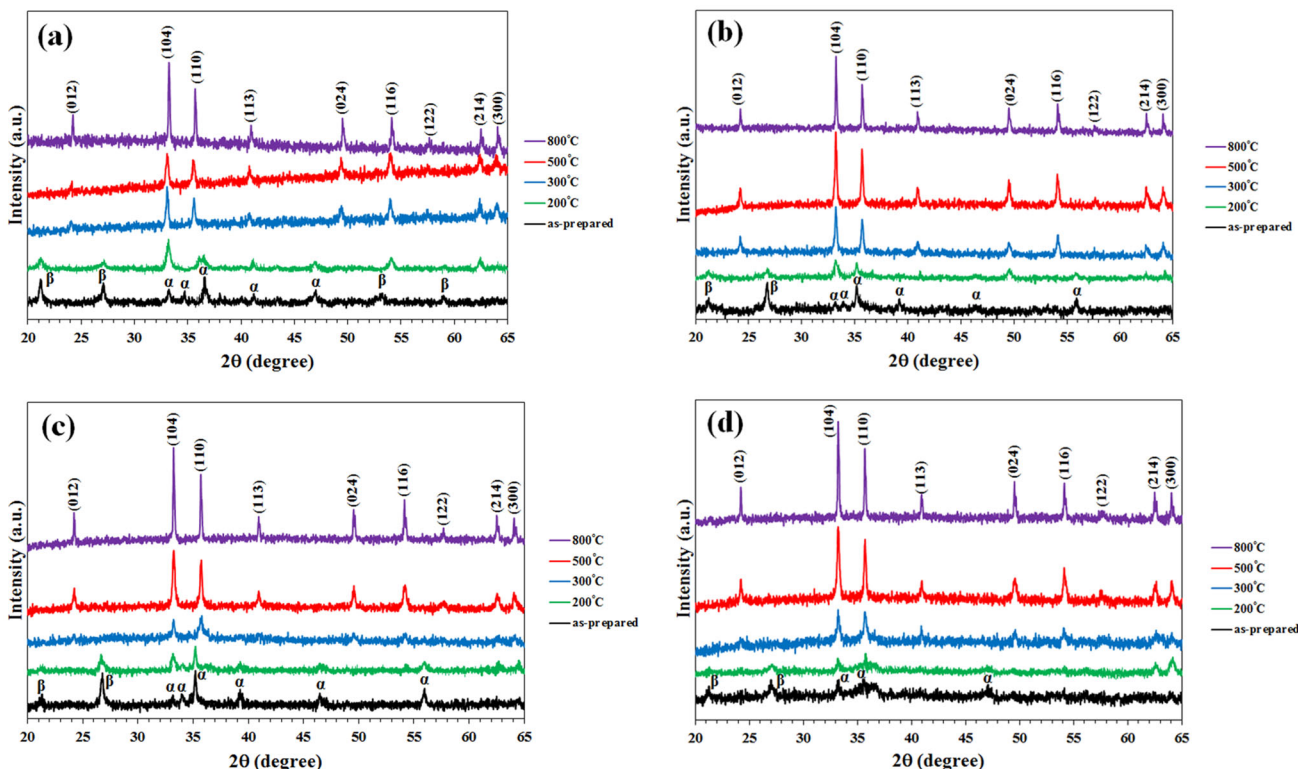


Fig. 1. XRD patterns of (a) $F_0$, (b) $F_1$, (c) $F_5$ and (d) $F_{10}$, before and after heat treatment at 200°C, 300°C, 500°C, and 800°C.
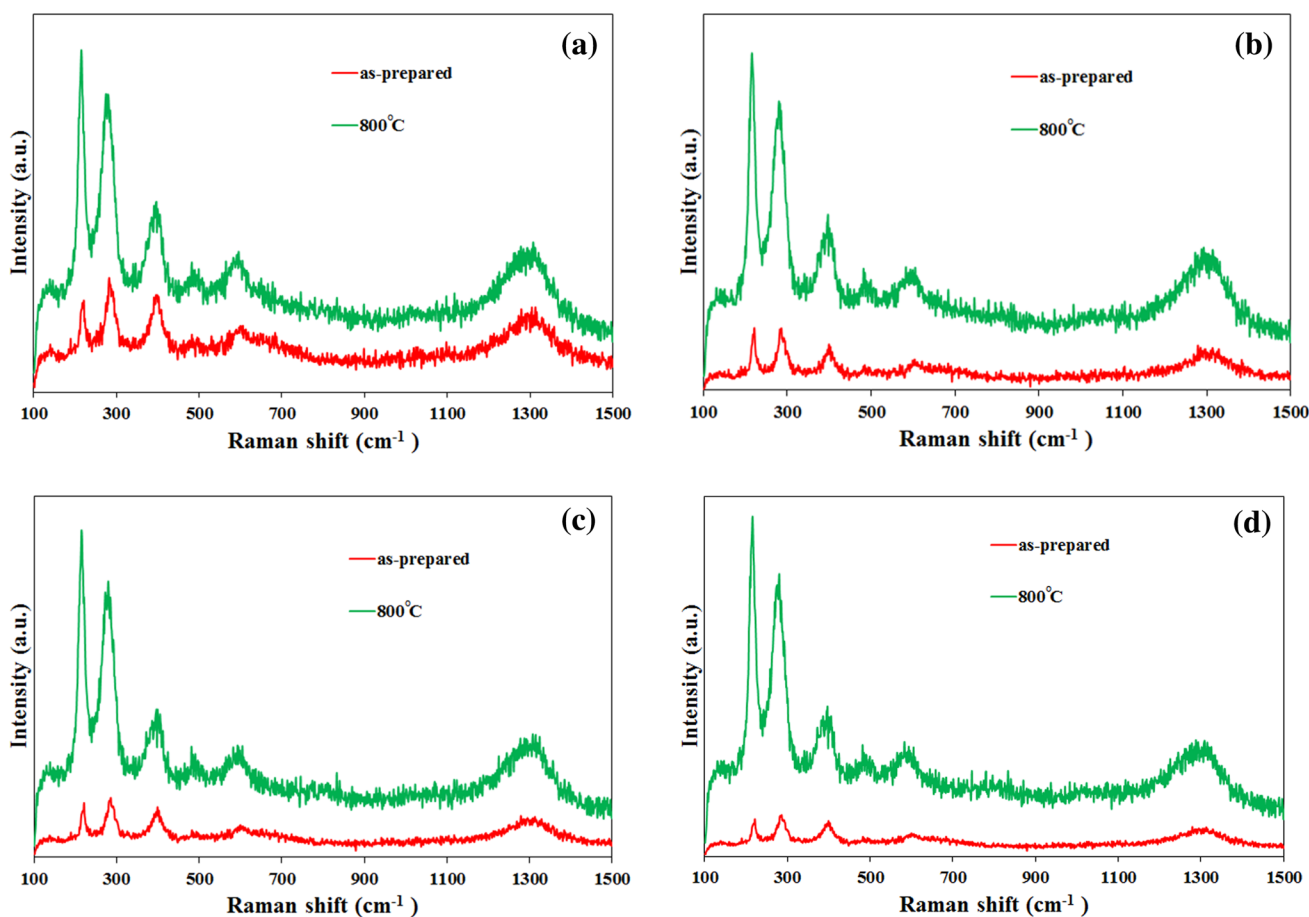
Fig. 2. Raman spectra of (a) $F_0$, (b) $F_1$, (c) $F_5$ and (d) $F_{10}$, before and after heat treatment at 800°C.

samples into the hematite phase and also increased their crystallinity (supplementary material: Fig. 1s). As expected, further heating to 800°C induced significant crystal growth of hematite, the only phase.[20] It is obvious from the XRD results that the as-prepared samples had poor crystallinity and yielded various peak intensities, whereas after heat treatment the particles were quite similar in crystallite structure.

## Raman Analysis

Raman spectroscopy of the as-prepared NPs indicated that they were composed of hematite and maghemite phases, the peaks at 215 cm$^{-1}$, 275 cm$^{-1}$, 595 cm$^{-1}$, and 1312 cm$^{-1}$ typically representing the hematite phase, while the peak at 384 cm$^{-1}$ represents the maghemite phase (Fig. 2).[7,23] Raman spectra revealed that, during heat treatment, the NPs started to transition from a mixed phase of $\gamma$ and $\alpha$ to a pure $\alpha$ phase. The observation of typical hematite peaks at 216 cm$^{-1}$, 282 cm$^{-1}$, 401 cm$^{-1}$, 486 cm$^{-1}$, 605 cm$^{-1}$ and 1306 cm$^{-1}$ demonstrated the complete transition of the NPs into the most stable phase. Furthermore,

Raman spectra of the annealed samples showed more intense and sharper peaks than those of the as-prepared samples,[7] demonstrating that heat treatment improved the crystallinity of the samples. These results are in agreement with the XRD measurements.

## FTIR Analysis

FTIR spectra were acquired for the as-prepared NPs and after heat treatment at 800°C (Fig. 3). Before heat treatment, two intense absorption peaks of the samples were observed at around 3360 cm$^{-1}$ and 1630 cm$^{-1}$, which can be respectively assigned to the symmetrical stretching and bending vibrations of the –OH groups.[7,23] The peaks at around 650 cm$^{-1}$ for the as-prepared samples can be assigned to the stretching mode of the Fe–O bonds in the tetrahedral site of the maghemite phase.[23,24] After heat treatment of the samples at 800°C, the –OH-related peaks of the $F_0$ and $F_1$ became broad and small, while in the FTIR spectra of the $F_5$ and $F_{10}$ the –OH-related peaks were totally absent and only two main broad metal–oxygen bands could be seen in the spectra. One peak

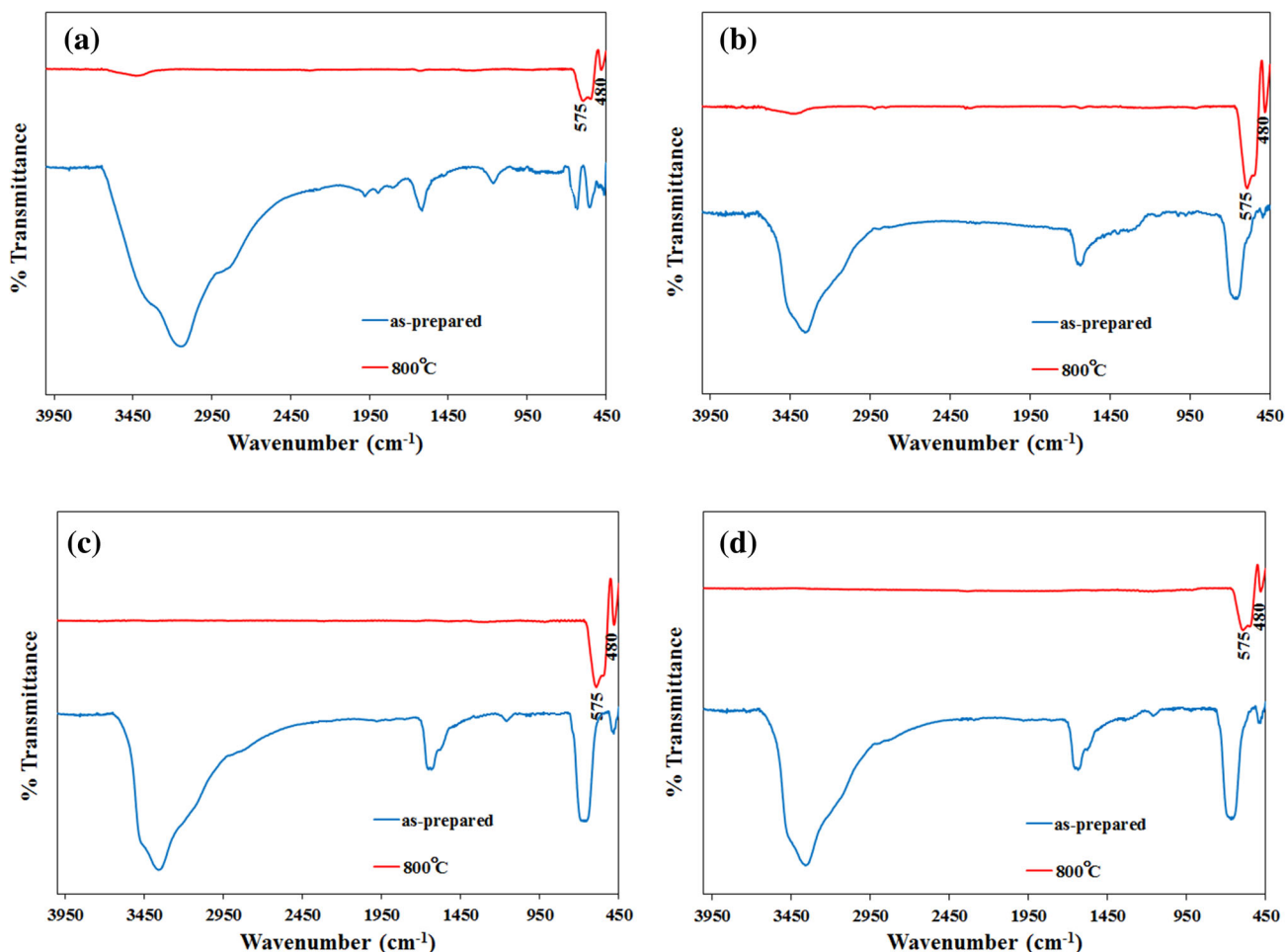Fig. 3. FT-IR spectra of (a) $F_0$, (b) $F_1$, (c) $F_5$ and (d) $F_{10}$, before and after heat treatment at 800°C.

observed at 575 cm$^{-1}$ corresponded to the intrinsic stretching vibration of the Fe–O, whereas another band, usually observed at 480 cm$^{-1}$, was assigned to the bending vibration of O–Fe–O in the hematite phase (supplementary material: Fig. 2s).[14,18,25] The observed phase transformation of the as-prepared samples after heat treatment was in agreement with the XRD and Raman results. Despite the different absorption peaks of the as-prepared samples, the FTIR patterns of all the annealed samples were almost similar.

## TEM Images

In our previous work, we mentioned that using different amounts of urea led to the formation of NPs of different shapes ($F_0$ particles were rod-shaped, $F_1$ particles were spindle-shaped, $F_5$ particles were ellipsoid and $F_{10}$ particles were flower-shaped) and sizes, which in turn led to differences in magnetic properties and other characteristics.[7,26] TEM images were acquired for all the samples after heat treatment at 800°C (Fig. 4). In the previous

paper, the effect of urea concentration on the shape and size of the particles was explained.[7] The sample prepared without urea ($F_0$) showed the greatest NP size, and the NP size decreased with increasing urea concentration. Careful analysis of the TEM images seemed to indicate some changes in the shape and size of the $Fe_2O_3$ NPs. These were probably due to the crystallization of the as-prepared NPs.[20] The TEM results showed that the size of the NPs was increased after heat treatment at 800°C,[12,27,28] and it was also apparent that the annealed particles had more regular and spherical shapes in comparison to the different particle shapes observed among the as-prepared samples.

## Magnetic Properties of $Fe_2O_3$ NPs

Figure 5 shows magnetic hysteresis curves of the $Fe_2O_3$ NPs (heated at various temperatures) measured by using a VSM in a maximum field of 10 kOe. As was reported in our previous work, magnetic hysteresis curves reveal that the as-prepared NPs had weak ferromagnetic behavior; no
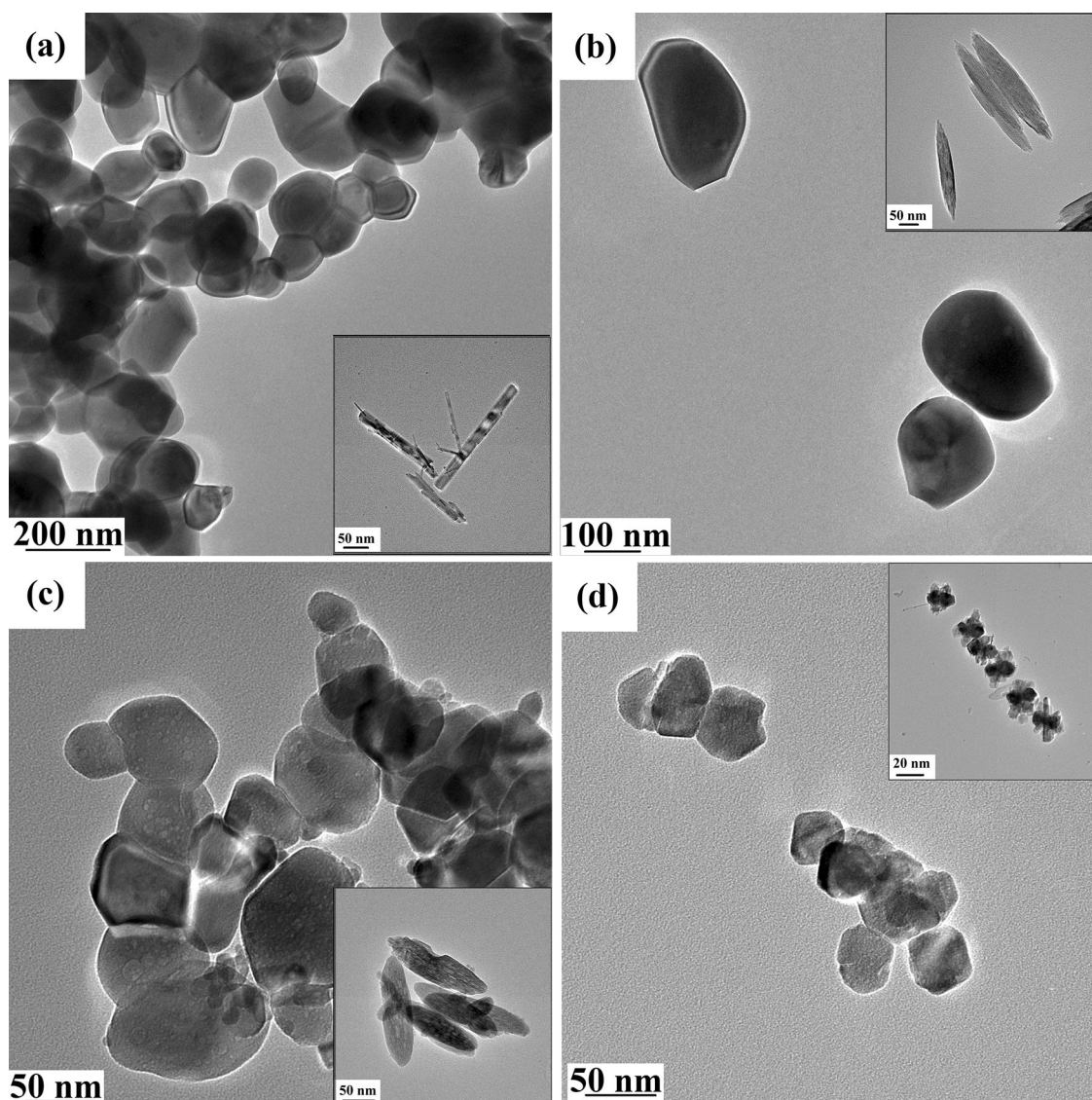
Fig. 4. TEM images of (a) $F_0$, (b) $F_1$, (c) $F_5$ and (d) $F_{10}$ NPs after heat treatment at 800°C (insets TEM of the samples before heat treatment).

saturation remanent magnetization ($M_r$) or coercive force ($H_c$) were observed for these samples.[7] The magnetization in $Fe_2O_3$ samples is dependent upon particle shape, and the reason for this is the symmetry and one-dimensional orientation of the atoms.[7,29–32] After heat treatment at different temperatures (Fig. 5), the samples showed drastic decreases in saturation magnetization ($M_s$). Despite the different values of $M_s$ observed for the as-prepared NPs,[7] $M_s$ was almost the same (0.10–0.16 emu/g) for all the annealed samples (Fig. 6). As mentioned before, magnetic properties strongly depend on particle shape. Before heat treatment, all the samples had different shapes, but after heat treatment at 800°C, they were all nearly spherical. Thus, it can be predicted that the similarity in $M_s$ among the annealed samples arose from their similar particle shapes.

## CONCLUSION

Heat treatment of MNPs has been introduced as a great technique to control magnetic properties of these NPs by affecting their shape, size and crystal structure. In this work, $Fe_2O_3$ NPs with different shapes were heated in the presence of air at 300°C, 500°C, and 800°C for 2 h. Both XRD and Raman spectroscopy results showed that, during heat treatment, the $Fe_2O_3$ NPs underwent the phase transformation from mixed $\alpha$- and $\gamma$- phases to hematite along with good crystallinity. TEM revealed changes in the size and morphology of the annealed samples, showing that the NPs became more regular and spherical during heat treatment. VSM data indicated that the as-prepared samples had better magnetic properties than the annealed samples.
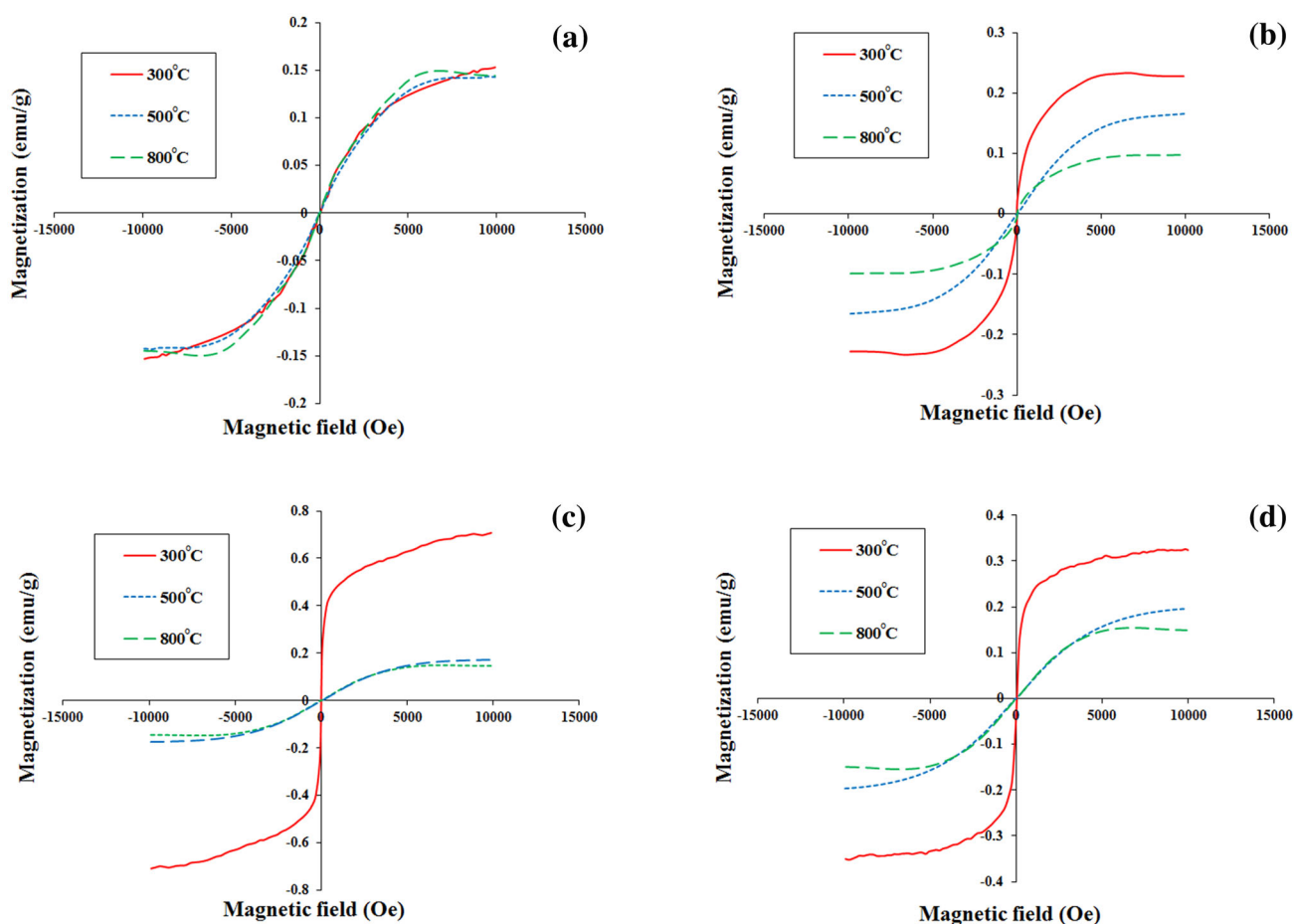
Fig. 5. Room-temperature magnetization curves of (a) $F_0$, (b) $F_1$, (c) $F_5$ and (d) $F_{10}$ NPs after heat treatment at 300°C, 500°C, and 800°C.
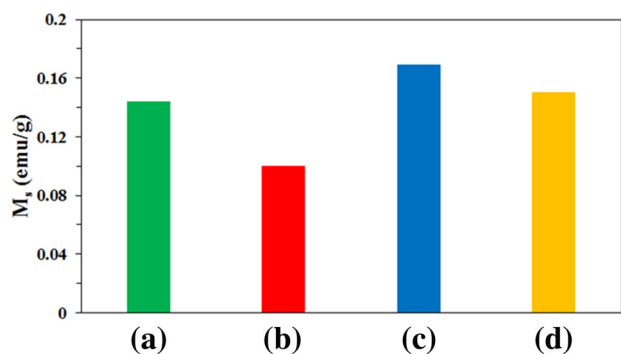


Fig. 6. Saturation magnetizations ($M_s$) of (a) $F_0$, (b) $F_1$, (c) $F_5$ and (d) $F_{10}$ NPs after heat treatment at 800°C.

**ELECTRONIC SUPPLEMENTARY MATERIAL**

The online version of this article (doi:10.1007/s11837-017-2429-0) contains supplementary material, which is available to authorized users.

**REFERENCES**

1. U. Topal and M.A. Aksan, *J. Magn. Magn. Mater.* 406, 123 (2016).
2. J.R. Jeong, S.J. Lee, J.D. Kim, and S.C. Shin, *Phys. Stat. Sol. (b)* 241, 1593 (2004).
3. B. Issa, I.M. Obaidat, B.A. Albiss, and Y. Haik, *Int. J. Mol. Sci.* 14, 21266 (2013).
4. A. Ito, M. Shinkai, H. Honda, and T. Kobayashi, *J. Biosci. Bioeng.* 100, 1 (2005).
5. A.H. Lu, E.L. Salabas, and F. Schuth, *Angew. Chem. Int. Ed.* 46, 1222 (2007).
6. A. Akbarzadeh, M. Samiei, and S. Davaran, *Nanoscale Res. Lett.* 7, 144 (2012).
7. S. Naghdi, K.Y. Rhee, B. Jaleh, and S.J. Park, *Appl. Surf. Sci.* 364, 686 (2016).

8. S. Layek, A. Pandey, A. Pandey, and H.C. Verma, *Int. J. Eng. Sci. Thechnol.* 2, 33 (2010).
9. E. Parsianpour, M. Gholami, N. Shahbazi, and F. Samavat, *Surf. Interface Anal.* 47, 612 (2015).
10. Y. Qu, H. Yang, N. Yang, Y. Fan, H. Zhu, and G. Zou, *Mater. Lett.* 60, 3548 (2006).
11. V. Viswanath, S. Maity, J.R. Bochinski, L.I. Clarke, and R.E. Gorga, *Macromolecules* 46, 8596 (2013).
12. S.R. Janasi, D. Rodrigues, and F.J.G. Landgraf, *Mater. Sci. Forum* 498, 119 (2005).
13. E.R. Kumar, T. Arunkumar, and T. Prakash, *Superlattices Microstruct.* 85, 530 (2015).
14. D.M. Yufanyi, A.M. Ondoh, J.F. Tendo, and K.J. Mbadcam, *Am. J. Chem.* 5, 1 (2015).
15. X.N. Xu, Y. Wolfus, A. Shaulov, Y. Yeshurun, I. Felner, I. Nowik, Y. Koltypin, and A. Gedanken, *J. Appl. Phys.* 91, 4611 (2002).
16. C. Vichery, I. Maurin, P. Bonville, J.P. Boilot, and T. Gacoin, *J. Phys. Chem. C* 116, 16311 (2012).
17. Y. Masubuchi, Y. Sato, A. Sawada, T. Motohashi, H. Kiyono, and S. Kikkawa, *J. Eur. Ceram. Soc.* 31, 2459 (2011).
18. S.K. Sahoo, K. Agarwal, A.K. Singh, B.G. Polke, and K.C. Raha, *Int. J. Eng. Sci. Thechnol.* 2, 118 (2010).
19. S.I.S. Ramya and C.K. Mahadevan, *Int. J. Res. Eng. Technol.* 3, 2321 (2014).
20. L. Stagi, J.A.D. Toro, A. Ardu, C. Cannas, A. Casu, S.S. Lee, and P.C. Ricci, *J. Phys. Chem. C* 5, 2857 (2014).
21. A.P. Swardhani, F. Iskandar, and M. Abdullah, *Advanced Materials Research*, Vol. 896 (Trans Tech Publications, 2014), pp. 100–103.
22. M. Tadic, M. Panjan, V. Damnjanovic, and I. Milosevic, *Appl. Surf. Sci.* 320, 183 (2014).
23. D. Chen, W. Wei, R. Wang, J. Zhua, and L. Guo, *New J. Chem.* 36, 1589 (2012).
24. S. Guo, G. Zhang, Y. Guo, and J.C. Yu, *Carbon* 60, 437 (2013).
25. S.Z. Mohammadi, M.K. Motlagh, S. Jahani, and M. Yousef, *Int. J. Nanosci. Nanotechnol.* 8, 87 (2012).
26. J.A. Schwarz, C.I. Contescu, and K. Putyera, *Dekker Encyclopedia of Nanoscience and Nanotechnology*, Vol. 3 (CRC press, 2004).
27. M. Ocan, M.P. Morales, and C.J. Serna, *J. Colloid Interface Sci.* 212, 317 (1999).
28. F.N. Sayed and V. Polshettiwar, *Sci. Rep.* 5, 9733 (2015).
29. S. Xuan, M. Chen, L. Hao, W. Jiang, X. Gong, Y. Hu, and Z. Chen, *J. Magn. Magn. Mater.* 320, 164 (2008).
30. X. Zhang, Y. Niu, Y. Li, X. Hou, Y. Wang, R. Bai, and J. Zhao, *Mater. Lett.* 99, 111 (2013).
31. Z. Liu, B. Lv, D. Wu, and Y. Sun, *Particuology* 10, 456 (2012).
32. X. Zhang, Y. Niu, Y. Yang, Y. Li, and J. Zhao, *New J. Chem.* 38, 4351 (2014).